

MIT Open Access Articles

*Characterization of a Novel Pyranopyridine Inhibitor
of the AcrAB Efflux Pump of Escherichia coli*

The MIT Faculty has made this article openly available. **Please share**
how this access benefits you. Your story matters.

Citation: Opperman, T. J., S. M. Kwasny, H.-S. Kim, S. T. Nguyen, C. Houseweart, S. D'Souza, G. C. Walker, N. P. Peet, H. Nikaido, and T. L. Bowlin. "Characterization of a Novel Pyranopyridine Inhibitor of the AcrAB Efflux Pump of Escherichia coli." *Antimicrobial Agents and Chemotherapy* 58, no. 2 (November 18, 2013): 722–733.

As Published: <http://dx.doi.org/10.1128/aac.01866-13>

Publisher: American Society for Microbiology

Persistent URL: <http://hdl.handle.net/1721.1/98344>

Version: Author's final manuscript: final author's manuscript post peer review, without publisher's formatting or copy editing

Terms of use: Creative Commons Attribution-Noncommercial-Share Alike



1 Title: Characterization of a novel pyranopyridine inhibitor of the AcrAB efflux pump of
2 *Escherichia coli*

4 Running title: Novel pyranopyridine efflux pump inhibitor

6 Keywords: efflux pump inhibitor, AcrAB, RND family, *Escherichia coli*, Enterobacteriaceae,
7 pyranopyridine

9 Authors:

10 Timothy J. Opperman^{1*}, Steven M. Kwasny¹, Hong-Suk Kim², Son Nguyen¹, Chad
11 Houseweart^{1†}, Sanjay D'Souza³, Graham C. Walker³, Norton P. Peet¹, Hiroshi Nikaido², and
12 Terry L. Bowlin¹

14 Affiliations:

15 ¹; Microbiotix, Inc., Worcester, MA 01605

16 ²; Department of Molecular & Cell Biology, University of California, Berkeley, CA 94720

17 ³; Department of Biology, Massachusetts Institute of Technology, Cambridge, MA 02139

18 †, deceased

20 *Corresponding Author:

21 Timothy J. Opperman

22 Microbiotix, Inc.

23 One Innovation Dr.

24 Worcester, MA 01605

25 508-757-2800

26 topperman@microbiotix.com

ABSTRACT

Members of the RND family of efflux pumps, such as AcrAB-TolC of *Escherichia coli*, play major roles in multi-drug resistance (MDR) in Gram-negative bacteria. A strategy to combat MDR is to develop efflux pump inhibitors (EPIs) for use in combination with an antibacterial agent. Here, we describe MBX2319, a novel pyranopyridine EPI with potent activity against RND efflux pumps of the Enterobacteriaceae. MBX2319 decreased the MICs of ciprofloxacin (CIP), levofloxacin, and piperacillin vs. *E. coli* AB1157 by 2-, 4-, and 8-fold, respectively, but did not exhibit antibacterial activity alone and was not active against AcrAB-TolC deficient strains. MBX2319 (3.13 μ M) in combination with 0.016 μ g/ml CIP (minimally bactericidal) decreased the viability (CFU/ml) of *E. coli* AB1157 by 10,000 fold after 4 h exposure, as compared to 0.016 μ g/ml CIP alone. In contrast, phenyl-arginine- β -naphthylamide (PA β N), a known EPI, did not increase the bactericidal activity of 0.016 μ g/ml CIP at concentrations as high as 100 μ M. MBX2319 increased intracellular accumulation of the fluorescent dye H33342 in WT, but not in AcrAB-TolC deficient strains, and did not perturb the transmembrane proton gradient. MBX2319 was broadly active against species of the Enterobacteriaceae and *Pseudomonas aeruginosa*. MBX2319 is a potent EPI with possible utility as an adjunctive therapeutic agent for the treatment of infections caused by Gram-negative pathogens.

INTRODUCTION

Multi-drug resistance (MDR) in Gram-negative pathogens, including the Enterobacteriaceae, *Pseudomonas aeruginosa*, *Acinetobacter spp.*, and *Stenotrophomonas maltophilia*, poses a significant threat to the effective treatment of infections caused by these organisms (1-4). The MDR threat has been exacerbated by the recent decrease in commercial efforts to discover and develop new antibacterial agents. In addition, antibacterial agents that have been introduced recently into the clinic, or are in development, such as daptomycin, gemifloxacin, telithromycin, and telavancin, are not active against Gram-negative pathogens. Recently FDA-approved agents with activity against Gram-negative bacteria include tigecycline and doripenem. While tigecycline is active against bacteria producing a tetracycline-specific pump *in vitro*, it is pumped out rapidly by the ubiquitous multidrug pumps, and its pharmacokinetic properties limit its use for treating urinary tract and bloodstream infections (5), as will the evolution of resistance during therapy (6). Clearly, novel strategies for effectively treating infections caused by MDR Gram-negative pathogens are urgently needed.

The MDR phenotype has been attributed to both acquired and intrinsic mechanisms of resistance. However, the RND efflux pumps of Gram-negative bacteria play a major role in MDR. Because of their broad substrate specificity, overexpression of these efflux pumps results in decreased susceptibility to diverse array of antibacterial agents and biocides (7). The major efflux pump of *E. coli* is a typical Resistance-Nodulation-Division (RND) pump, which is a tripartite structure consisting of an integral membrane efflux transporter with broad substrate specificity (AcrB), an outer membrane channel (TolC), and a periplasmic protein adapter (AcrA). Antibiotics enter the periplasmic space through a porin or by diffusion through the lipid bilayer, where they interact with the substrate binding pocket of AcrB. The AcrB transporter uses proton motive force to extrude the compound into the TolC channel and to the exterior (8). These RND family pumps not only produce intrinsic levels of resistance to antibacterial agents, including the

fluoroquinolones (FQs; e.g. ciprofloxacin and levofloxacin), β -lactams (e.g. piperacillin, meropenem, and aztreonam) (9), and β -lactamase inhibitors (e.g. clavulanate and sulbactam) (10, 11), but also produce an MDR phenotype when overproduced (29). In addition, elimination of RND pumps in *P. aeruginosa* by genetic deletion (12) or inhibition with a potent EPI (13) decreases the frequency of resistance to levofloxacin. In *E. coli*, a functional AcrAB-TolC is required for the selection of mutations in the targets of FQs (*gyrA* and *gyrB*) that give rise to FQ resistance (14). Furthermore, RND pumps have been shown to play a role in virulence of the enteric pathogen *Salmonella enterica* serovar Typhimurium (15), and EPIs that target RND pumps have been shown to inhibit biofilm formation in *E. coli* and *K. pneumoniae* (16). Therefore, EPIs could be used as adjunctive therapies with an FQ or β -lactam antibiotic to improve antibacterial potency at low antibiotic concentrations, reduce the emergence of resistance, inhibit biofilm formation, and decrease virulence of enteric pathogens.

Several potent efflux pump inhibitors have been described in the literature (17), however, none have reached clinical development. A family of peptidomimetics, including PA β N (MC-207 110), that exhibited potent inhibition of efflux pumps in *P. aeruginosa* has been developed for use as an adjunctive therapy (13, 18-22). Some of these inhibitors were validated using *in vivo* infection models (19, 20, 22), however, they were abandoned because of toxicity (23). In addition, a series of pyridopyrimidine EPIs that are specific for the MexAB efflux pump of *P. aeruginosa* was advanced to the preclinical stage (24-30). In this paper, we describe the discovery and *in vitro* characterization of MBX2319, a novel **pyranopyridine** inhibitor of RND-class AcrAB-TolC efflux pump in *E. coli* and other pathogens of the Enterobacteriaceae.

MATERIALS AND METHODS

Strains and reagents. The strains used in this study are listed in Table 1. The following strains were obtained from the Keio collection (31): JW0451 (Δ *acrB*::kan), JW5503 (Δ *tolC*::kan),

JW3234 (Δ *acrF*::kan), JW2661 (Δ *emrB*::kan), JW0863 (Δ *macB*::kan). The deletion mutations in each of these strains were transferred to AB1157 using P1 phage transduction (see Table 1). The construction of the *E. coli* cell-based reporter strain (SOS-1) that was used for high throughput screening is described in detail in the supplementary information. Ciprofloxacin was purchased from ICN Biomedicals (Aurora, OH). Irgasan was a generous gift from Ciba Speciality Chemicals, Inc. (High Point, NC). Hoechst 33342 (H33342) was purchased from Molecular Probes (Eugene, OR). The following reagents were purchased from Sigma Aldrich (St. Louis, MO): phenyl-arginine- β -naphthylamide (PA β N), cyanide-m-chlorophenyl hydrazone (CCCP), levofloxacin, norfloxacin, naladixic acid, piperacillin, cloxacillin, oxacillin, cloramphenicol, tetracycline, ethidium bromide, gentamicin, crystal violet, cephalixin, amoxicillin, rifampicin, cefotaxime, carbenicillin, novobiocin, erythromycin, linezolid, acriflavine, chlorhexidine, benzalkonium chloride, and cetylpyridinium chloride.. [*methyl*-³H] β -D-thiogalactopyranoside ([³H] TMG; 1 mCi/ml, 7 Ci/mmol) was obtained from Moravek Biochemicals (Brea, CA). Luria Broth (Miller) and agar were purchased as prepared dehydrated media from Becton Dickinson (Franklin Lakes, NJ). The compound libraries used in high-throughput screens were purchased from Chembridge (San Diego, CA), ChemDiv (San Diego, CA), and TimTec (Newark, DE).

Chemistry. The synthesis of MBX2319 is described in the Supplementary Information.

Antibacterial activity assays. The minimal inhibitory concentration (MIC) of antibacterial agents and biocides was determined using the microbroth dilution method essentially as described in the CLSI protocol M7-A7 (32), with the following exceptions. LB media was used instead of MHB. Serial two-fold dilutions of test compounds were made in DMSO at concentrations 50-fold higher than the final concentration: the diluted compounds were added to the assay plates, and 100 μ l of the bacterial culture was added to each well. The final concentration of DMSO in each assay was 2%. When indicated, MIC assays were performed in the presence of an efflux

pump inhibitor (EPI) at a final concentration of 25 μ M. MIC assays were performed in triplicate and the geometric mean was calculated. Checkerboard MIC assays using an EPI and an antibacterial agent were performed essentially as described (33), with the same modifications used for the MIC assays described above.

Time-kill assays. Killing curve assays were performed essentially as described (33).

Exponential bacterial cultures grown in LB were diluted to a cell density of $\sim 1 \times 10^7$ in LB followed by addition of CIP and/or an EPI. Viability was monitored over 2-4 hours by making serial dilutions in saline and spotting 5 μ l of each dilution onto the surface of an LB agar plate in triplicate. Colonies were counted after the plates were incubated at 37 $^{\circ}$ C for 16-18 h, colony forming units (CFU) per ml were calculated, and the average and standard deviation for the three replicates was determined. For treatments that decreased CFU/ml below the limit of detection for the spot plating method, the 100 μ l samples were diluted into 5 ml LB top agar, poured onto LB agar plates, and incubated for 18 h at 37 $^{\circ}$ C. To calculate the fraction of the control for each sample, the average CFU/ml values for treated samples were divided by those from the same sample at 0 h (time = 0). Each experiment was repeated at least three times, and a representative experiment is shown.

H33342 accumulation assay. The H33342 accumulation assay was used to evaluate the effect of EPIs on the activity of the AcrAB-TolC efflux pump in several bacterial species essentially as described (34). Briefly, bacterial cultures were grown overnight in LB (Miller) with aeration at 37 $^{\circ}$ C and were used to inoculate fresh cultures (1:100 dilution) that were grown in LB (Miller) with aeration until an optical density at 600 nm (OD_{600}) of 0.4-0.6 was reached. Bacterial cells were harvested by centrifugation, and the cell pellet was washed with a volume of PBSM+G (PBS containing 1 mM $MgSO_4$ and 20 mM glucose) equivalent to the original volume of the culture. After centrifugation, the cell pellets were resuspended in PBSM+G and the OD_{600} of each suspension was adjusted to 0.2. Aliquots of 190 μ l were transferred to the wells of a 96-well

assay plate (Costar 3515, Corning, NY; flat bottom, black plate). Various concentrations of test compounds dissolved in DMSO or an equivalent volume of solvent alone were added to a total of 8 assay wells (one column of wells) for each condition tested. The final concentration of DMSO in all assays was 2%. The assay plates were incubated at 37 °C for 15 min, and 10 µl of a solution of 50 µM H33342 in PBSM+G was added to each assay well, resulting in a final dye concentration of 2.5 µM. Fluorescence (excitation and emission filter of 355 and 460 nm, respectively) of each well was measured at 37 °C every 5 min for 30 min using a Victor² V 1420 Multilabel HTS Counter (Perkin Elmer, Waltham, MA). The average values and standard deviations for the eight replicates for each condition were calculated using Microsoft Excel. Each experiment was repeated at least three times, and a representative experiment is shown.

Kinetics of nitrocefin efflux by AcrAB-TolC in E. coli. The effects of EPIs on the kinetic parameters of AcrAB-TolC in *E. coli* were estimated as described (35). Briefly, HN1157 was grown in modified LB broth, diluted 100-fold in the fresh medium, and incubated at 30 °C with shaking until the OD₆₀₀ reached 0.65. The cells were harvested, washed twice (50 mM potassium phosphate buffer, pH 7.0, 5 mM MgCl₂), and resuspended in the same buffer at an OD₆₀₀ of 0.8 (corresponding to 0.24 mg dry weight/mL). Nitrocefin was added at a desired final concentration and the mixture incubated at 25 °C while OD₄₈₆ was measured over 30 min. The concentration of nitrocefin in the periplasm (C_p) was calculated from the rate of hydrolysis by the periplasmic β -lactamase (V_h) and the kinetic constants of the β -lactamase as described (35). The kinetic constants were derived by curve fitting of the velocity of AcrB (V_e) vs. C_p values using GraphPad Prism, version 5.04 (<http://www.graphpad.com/>) by using the Michaelis-Menten equation. Each assay was repeated at least three times, and representative data are presented.

Uptake of [3H]-TMG by the LacY permease. To estimate the effect of EPIs on the proton motive force in *E. coli* HN1157, the accumulation of [3H]-TMG by the LacY permease was

measured essentially as described (36). Briefly, a culture of HN1157 was grown in LB medium containing 1 mM of isopropyl β -D-1-thiogalactopyranoside (IPTG) at 30 °C with shaking, was harvested at an OD₆₀₀ of ca. 0.65, and washed two times with 50 mM KHPO₄ buffer, pH 7.0, 5mM MgCl₂ (PBB). The cells were resuspended in PBB and the OD₆₀₀ was adjusted to 0.8. The cell suspension was used immediately without the further addition of an energy source. To 1 ml of cell suspension, 5 μ l of test compound solution (final concentration of 0.2, 2 and 20 μ M), or 20 mM CCCP (final 100 μ M; negative control), or DMSO (positive control) was added and preincubated for 10 min at room temperature. Then, an aliquot of 250 μ l of cells was removed and added to 5 μ l of a 12.5 mM [³H]TMG solution (final concentration, 0.25 mM; 2 μ Ci/ μ mol). After further incubation for 10 min, aliquots (200 μ l) were removed and filtered on a 25-mm-diameter 0.45 μ m HA filter (Millipore, Billerica, MA). The filters were washed two times with 5 ml of PBB and counted with 5 ml of EcoLume scintillation cocktail (ICN Biomedicals, Costa Mesa, CA) in a TM Analytic, Delta 300 liquid scintillation counting system model 6891 (Elk Grove Village, IL).

Outer membrane integrity assay. HN1157 was grown in modified LB broth + 5 mM MgSO₄, diluted 500-fold in LB, and incubated at 30 °C with shaking until the OD₆₀₀ reached 0.65. The cells were harvested, washed twice (50 mM potassium phosphate buffer, pH 7.0), and resuspended in the same buffer at an OD₆₀₀ of 0.65. The cell suspension was transferred to the wells of an assay plate containing compound or solvent, nitrocefin was added at final concentration of 75 μ M, OD₄₈₆ was measured over 20 min, and the velocity of hydrolysis (V_h) was calculated.

Cytotoxicity assay. The cytotoxicity of MBX2319 against a mammalian cell line (HeLa, ATCC CCL-2) was determined as described (37). The compound concentration that inhibits the conversion of vital stain MTT to formazan by 50% (CC₅₀), as compared to an untreated control, was determined using the 4-parameter curve-fitting program contained in GraphPad Prism,

version 5.04 (<http://www.graphpad.com/>). The assay was performed in triplicate in at least two separate experiments.

RESULTS.

Identification of MBX2319. To identify compounds that act synergistically with ciprofloxacin (CIP), we developed a cell-based reporter assay that reports on both SOS induction and viability. Using the cell-based reporter assay, we screened 183,400 compounds, and identified 1,782 primary hits, which were evaluated in a panel of secondary assays for prioritization based on potency and specificity. The details of the screening and secondary assays will be published elsewhere. Based on the results of these analyses, MBX2319 (Fig. 1) was chosen for further study.

*MBX2319 potentiates the antibacterial activity of fluoroquinolone and β -lactam antibiotics against *E. coli*.* We utilized a checkerboard assay to determine whether MBX2319 potentiates the activity of two fluoroquinolones, ciprofloxacin (CIP) and levofloxacin (LEV), and a β -lactam, piperacillin (PIP), against *E. coli* AB1157. The results, shown in Table 2, demonstrate that MBX2319 at 12.5 μ M decreases the MICs of CIP, LEV, and PIP by 2, 4, and 8-fold, respectively. MBX2319 alone did not exhibit antibacterial activity (MIC \geq 100 μ M). In addition, MBX2319 increased the bactericidal activity of 0.016 μ g/ml CIP (1 \times MIC), which is minimally bactericidal against *E. coli* AB1157, in a dose-dependent manner (Fig. 2A). The highest concentration of MBX2319 (3.13 μ M) decreased viability (CFU/ml) by 10,000 fold after 4 h exposure, as compared to 1 \times MIC CIP alone. In contrast, MBX2319 alone at concentrations up to 50 μ M did not affect growth. As a comparison, we measured the effect of various concentrations of phenyl-arginine- β -naphthylamide (PA β N), a known EPI (13), in combination with 0.016 μ g/ml CIP in the time kill assay. The results of the assay are shown in Fig. 2B, and demonstrate that PA β N at concentrations as high as 100 μ M did not increase the bactericidal activity of 0.016 μ g/ml CIP. This finding is consistent with a previous report that showed that

PA β N at a concentration of 25 mg/ml (48 μ M) had a limited effect on the antibacterial of fluoroquinolones against Enterobacteriaceae (38).

MBX2319 is an efflux pump inhibitor (EPI). To verify that the mechanism by which MBX2319 potentiates the antibacterial activity of fluoroquinolones and β -lactams is through inhibition of efflux, we determined whether MBX2319 potentiated the antibacterial activity of CIP, LEV, and PIP against a panel of efflux-defective mutants of *E. coli* AB1157. We reasoned that the antibiotic sensitivity of mutants lacking the target of MBX2319 would not be affected by the compound. The results of a checkerboard assay, shown in Table 2, demonstrate that the MICs for the $\Delta tolC$ and $\Delta acrB$ mutants were not affected by MBX2319, whereas, mutants defective in other pumps that interact with TolC, such as AcrF (Table 2), MacB, and EmrB (data not shown) exhibited MIC shifts similar to those of WT (AB1157). Similarly, MBX2319 potentiated the bactericidal activity of CIP against the $\Delta acrF$ strain, but not against $\Delta tolC$ and $\Delta acrB$ strains (Fig 2C). Finally, MBX2319 potentiated the antibacterial activity of CIP, LEV, and PIP by 4-8 fold against *E. coli* strains 285 and 287 (Table 2), which are CIP^R mutants of *E. coli* AB1157 that were selected during a serial passage in subinhibitory concentrations of CIP, and exhibit increased efflux activity (see supplementary material). Significantly, MBX2319 reduced the MICs against *E. coli* strains 285 and 287 to levels that are comparable to those obtained against isogenic efflux-defective mutants ($\Delta tolC$). These findings indicate that the AcrAB-TolC efflux pump, which is the major efflux pump in *E. coli* (39), is a target of MBX2319. However, because deletion mutations of *acrF*, *acrD*, *macB* and *emrB* do not affect susceptibility to the antibiotics used in this study, our results do not rule out the possibility that MBX2319 also inhibits the efflux pumps encoded by these genes.

To confirm MBX2319 directly inhibits efflux, we used an assay that measures the accumulation of the fluorescent DNA-binding dye Hoechst 33342 (H33342), which is a substrate of the AcrAB-TolC pump, in *E. coli* AB1157 (34). This assay has been used to estimate efflux activity in *E.*

coli and *S. enterica* (34). When H33342 enters the cell it binds to the DNA minor groove, becomes fluorescent, and can be detected using a fluorescent plate reader (Ex355, Em460). Efflux-competent cells extrude H33342 and accumulate the dye at a relatively slow rate, resulting in low levels of fluorescence. Conversely, efflux-defective cells accumulate intracellular levels of H33342 at a higher rate, resulting in increased levels of fluorescence. The results of the H33342 accumulation assay are shown in Fig 3A and B. The $\Delta acrB$ strain was used as a positive control, indicating the maximum levels of H33342 accumulation possible. MBX2319 (Fig. 3A) and PA β N (Fig 3B) increased accumulation of H33342 as compared to the untreated control in a dose-dependent manner, although not linearly for MBX2319 at higher concentrations (25 – 50 μ M) approaching the aqueous solubility limit. MBX2319 did not increase accumulation of H33342 in the $\Delta acrB$ and $\Delta tolC$ strains (Fig. 3C), which is consistent with the hypothesis that AcrAB-TolC is the target. At a concentration of 25 μ M, MBX2319 and PA β N increased H33342 accumulation to levels that were about 45% and 52% of the $\Delta acrB$ strain, respectively. MBX2319 was more effective in this assay at lower concentrations (3.1-12.5 μ M) than was PA β N. Both compounds increased H33342 accumulation in the hyper-efflux strains 285 and 287 (see Fig. 3D).

Finally, we measured the effect of MBX2319 and PA β N on the real-time efflux of nitrocefin by the AcrB efflux pump in intact cells (35). This assay measures the rate of nitrocefin hydrolysis by the AmpC β -lactamase as a function of the external nitrocefin concentration to estimate the periplasmic concentration (C_p) of nitrocefin, which can be used to estimate the K_m and V_{max} for the AcrAB-TolC efflux pump. The assay was repeated 12 times with and without 0.2 μ M MBX2319 and a clear inhibition of efflux was seen in all cases except one. A typical data is shown in Fig. 4A, in which curve-fitting suggests that most of the inhibition occurred by a large (4.4-fold) increase in K_m . Although the curve-fitting also suggested that there was a marginal (2-fold) increase in V_{max} , this is of uncertain significance because the fitting had to be done in a

quasi-linear range of the plot. In most other assays, MBX2319 caused little changes in V_{max} (not shown). These data are consistent with the notion that MBX2319 competes with nitrocefin for the binding site, or decreases access to binding site. Higher concentrations of MBX2319 (1 - 10 μ M) completely inhibited nitrocefin efflux and prevented kinetic analyses. In contrast, PA β N at concentrations ranging from 0.2 to 10 μ M had no effect on the efflux of nitrocefin, suggesting that this compound does not directly affect AcrB function at this range of concentrations. A representative result for an assay performed using 1 μ M PA β N is shown in Fig. 4B.

MBX2319 potentiates multiple antibiotics and biocides. Efflux pump inhibitors are known to increase the antibacterial activity of a diverse group of antibiotics and biocides. To test this prediction, we measured the ability of MBX2319 to increase the susceptibility of *E. coli* AB1157 to a broad spectrum of antibiotics and biocides. The data, shown in Table 3, demonstrate that MBX2319 increased susceptibility to several known AcrAB-TolC substrates, such as CIP, LEV, nalidixic acid, PIP, oxacillin, and chloramphenicol, but not to gentamicin and carbenicillin, which are not substrates (40). In general, the MIC shifts produced by MBX2319 were lower than those of the Δ *acrB* and Δ *tolC* strains, but were similar to those produced by PA β N for fluoroquinolone and β -lactam antibiotics. Interestingly, the MIC shifts produced by PA β N for rifampicin and was greater than that of the Δ *acrB* strain, suggesting an additional mechanism of action for PA β N.

MBX2319 does not perturb bacterial membranes. Because the AcrAB-TolC efflux pump utilizes proton motive force (41), compounds that perturb the proton gradient across the cytoplasmic membrane can inhibit efflux through an indirect mechanism. To determine whether MBX2319 perturbs the transmembrane proton gradient, we measured uptake and accumulation in the presence of MBX2319 of 3 H-TMG by the LacY permease, which requires proton motive force (42). The results are shown in Table 4. MBX2319 did not significantly inhibit uptake and accumulation of 3 H-TMG at concentrations up to \sim 20 μ M and thus, does not inhibit efflux indirectly by perturbing the proton gradient.

PA β N has been shown to affect the integrity of the outer membrane, which is predicted to increase the rate of permeation of antibiotics into the periplasm (13). To determine whether MBX2319 affects the permeability of the outer membrane, we measured the influx of nitrocefin in a strain deficient in AcrAB (HN1159). The data, shown in Table S3 (supplementary material), demonstrate that 20 μ M MBX2319 does not increase the rate of nitrocefin influx, indicating no effect on outer membrane permeability.

Spectrum of activity. To determine whether MBX2319 inhibits the AcrAB-TolC orthologs of other Gram-negative pathogens, we measured the antibacterial activity of MBX2319 in combination with several antibiotics using three assays. First, we measured the MICs of several antibiotics, alone or in combination with MBX2319 or PA β N at a concentration of 25 μ M against several Gram-negative pathogens. The data are shown in Table 5. MBX2319 increased significantly the activity of CIP and LEV against the majority of the organisms tested, whereas, PA β N (25 μ M) did not significantly affect the MICs. MBX2319 and PA β N increased the activity of PIP and CEF against the majority of organisms tested, however, MBX2319 was active against more organisms than was PA β N. In addition, MBX2319 increased the activity of CIP and LEV against *E. coli* 331, which is resistant to fluoroquinolones. MBX2319 was not effective against *Proteus mirabilis* or any of the antibiotics tested (data not shown).

Second, a time kill assay was used to verify the potentiating activity of 25 μ M MBX2319 against Gram-negative pathogens (Fig. 2D). The combination of MBX2319 and a minimally bactericidal concentration of CIP (0.5 or 1 \times MIC) decreased viability of *Shigella flexneri*, *Salmonella enterica*, *Enterobacter aerogenes*, and *Klebsiella pneumoniae*, by 100-1000 fold as compared to CIP alone. In contrast, 25 μ M PA β N was not effective against any of the strains tested in this assay. Third, the H33342 accumulation assay was used to verify that MBX2319 inhibits efflux in other Gram-negative pathogens. The results of this assay are shown in Fig. 5A-H. MBX2319 (25 μ M) increased H33342 accumulation in the majority of organisms tested, including *Shigella*

flexneri, *K. pneumoniae*, *S. enterica*, *E. cloacae*, and showed weak activity against *E. coli* (CIP^R), *P. mirabilis*, and *P. aeruginosa*.

MBX2319 increases antibacterial activity of levofloxacin and piperacillin against a diverse panel of E. coli strains. To determine whether MBX2319 increases the antibacterial activity of LEV and PIP against a diverse panel of *E. coli* strains, we measured MICs for LEV and PIP in the absence and presence of 25 μ M compound. The panel of 24 strains (see Table S4) is comprised of strains that were publicly available clinical isolates; however, none of the strains was resistant to high levels of fluoroquinolones. Because the spectrum of activity includes the pathogens that are prevalent in urinary tract infections (UTI), the *E. coli* panel included several strains isolated from UTIs. MBX2319 decreased the MIC₅₀ and MIC₉₀ for LEV (the concentration of LEV that inhibits growth of 50% and 90% of the strains, respectively) by four fold (Fig. 6). In contrast, MBX2319 did not have a significant effect on the MIC₅₀ or MIC₉₀ for PIP, probably because ~20% of strains appeared to be resistant to PIP, as evidenced by the plateau in the cumulative % susceptible at ~80%, which is likely to be the result of β -lactamase expression.

Cytotoxicity. The cytotoxicity of MBX2319 against HeLa cells was determined as described (37). The concentration of compound that reduced cell viability by 50%, or CC₅₀, was determined using a four parameter curve fitting algorithm (GraphPad Prism). The CC₅₀ for MBX2319 against HeLa cells was $\geq 100 \mu$ M, however, it is possible that the apparent lack of cytotoxicity is due, at least in part, to the relatively low aqueous solubility of this compound.

DISCUSSION.

In this report, we describe the preliminary *in vitro* characterization of MBX2319, a novel inhibitor of the RND-class AcrAB-TolC efflux pump, which is the major efflux pump in *E. coli* and other Enterobacteriaceae and plays a major role in the MDR phenotype of these pathogens (7). Our results demonstrate that MBX2319 exhibits the following characteristics of an EPI, as described

by Lomovskaya *et al.* (13): 1) Potentiates the antibacterial activity of diverse agents that are substrates of AcrAB-TolC, 2) Does not potentiate the antibacterial activity of agents that are not substrates, 3) Does not exhibit activity against mutants lacking functional AcrAB-TolC pumps, 4) Inhibits the extrusion or accumulation of AcrAB-TolC substrates, and 5) Does not affect the energy source of AcrAB-TolC (proton gradient).

The most likely mechanism of inhibition of MBX2319 is through competitive inhibition and/or by blocking access to the substrate binding site of AcrB. However, our data does not rule out the possibility that MBX2319 inhibits other RND pumps, such as AcrF. The substrate binding pocket of AcrB is large and flexible, and is rich in phenylalanine residues that define the binding pocket and interact with substrate molecules via hydrophobic and ring stacking interactions (43, 44). Docking studies suggested that different pump substrates bind to distinct sites in the substrate binding pocket (45). However, it was unclear how inhibitors, such as PA β N or 1-(1-naphthylmethyl)-piperazine (NMP), could inhibit the extrusion of multiple chemically distinct substrates. The results of MD simulations (46) suggested that PA β N and NMP interact with the “G loop” (aka switch loop), which separates the access site and the substrate binding pocket. The G-loop is predicted to move substrates to the distal binding pocket through peristaltic action. Mutations that are predicted to prevent movement of the loop (G614P+G621P and G616P+G619P) abolished efflux of doxorubicin and increased the sensitivity of the mutant strain to erythromycin (47). Therefore, efflux pump inhibitors could inhibit the efflux of diverse substrates by AcrB through binding to the G-loop. However, differences in the spectrum of compounds potentiated by MBX2319 as compared to PA β N suggest that MBX2319 binds to a different site in the AcrB binding pocket. Experiments that will further define the mechanism of MBX2319 are underway in our laboratories.

The pyranopyridine MBX2319 appears to be a novel EPI, as it is not similar structurally to any of the EPIs that have been described previously. However, a comparison of the structures of

370 MBX2319 and other EPIs, such as the peptidomimetic PA β N and pyridopyrimidine D13-9001
371 (29), reveals that these potent EPIs contain at least two hydrophobic ring systems that
372 presumably interact with hydrophobic residues in the substrate binding site. The activity
373 exhibited by MBX2319 in *in vitro* assays was comparable or superior to that of PA β N at the
374 same concentrations. Unlike PA β N, the activity of MBX2319 was not dependent on the
375 presence of primary amines, which were required for activity and were responsible for the
376 toxicity of PA β N and later analogs (23). The mechanism of action of MBX2319 appears to be
377 through the exclusive inhibition of AcrAB-TolC, as compared to PA β N, which also increases the
378 permeability of the outer membrane (13). This additional mechanism was apparent in the
379 potentiation of rifampicin to levels that are greater than those of an Δ *acrB* strain (see Table 3).
380 Finally, MBX2319 possesses several drug-like properties: molecular weight (409.54), clogP
381 (4.03), number of hydrogen bonding acceptors (5), number of hydrogen bonding donors (0),
382 polar surface area (45.49 Å²), and rotatable bonds (2). We are currently exploring structure-
383 activity relationship of this novel scaffold to develop analogs with improved activity.

384 MBX-2319 is active against *E. coli* and other Gram-negative pathogens of the
385 Enterobacteriaceae, including *Shigella flexneri*, *K. pneumoniae*, *S. enterica*, *E. cloacae*. In
386 addition, MBX2319 significantly decreased the MICs for FQs against fluoroquinolone resistant
387 strains of *E. coli* (strains 331, 285, 287), but it did not overcome resistance caused by mutations
388 in the FQ target. These results indicate a potential for broad spectrum activity against
389 pathogens of the Enterobacteriaceae. The majority of published EPIs are not active against the
390 MexAB-OprM efflux pump of *P. aeruginosa* (48), with the notable exceptions of PA β N (13) and
391 DS-9001 (29), which exhibit activity against this pump. However, MBX2319 exhibited limited,
392 but significant, activity against *P. aeruginosa*, suggesting that it may be possible to develop
393 analogs with an extended spectrum of activity. AcrB and MexB are very similar in both primary
394 (69.8% identity and 83.2% similarity) and three-dimensional structure (rmsd of 1.4 Å) (49).

395 However, subtle differences in primary and tertiary structure appear to underlie the observed
396 differences in substrate specificity (50). Because of the similarities that exist in the remainder of
397 the substrate binding pocket, it may be possible to design analogs of MBX2319 with improved
398 potency against MexB. Attempts to identify the potential sites of interaction of MBX2319 are
399 underway.

400 Recent reports have underlined the importance of RND family efflux pumps in the MDR
401 phenotype (7), and in resistance to fluoroquinolones and β -lactams, in particular. MBX2319
402 potentiated the activity of fluoroquinolone and β -lactam antibiotics against *E. coli* and other
403 important enterobacterial pathogens, such as *Shigella flexneri*, *Salmonella enterica* (serovar
404 Typhimurium), *Enterobacter aerogenes*, *E. cloacae* (data not shown) and *Klebsiella*
405 *pneumoniae*, that utilize RND-family pumps. In addition, MBX2319 potentiated the activity of
406 the CIP and LEV against *P. aeruginosa* PA01, a laboratory strain, but not against the reference
407 strain ATCC 27854. However, the MIC of CEF against ATCC 27854 was decreased
408 significantly (~6-fold) by MBX2319. Taken together, the data suggest that MBX2319 has the
409 potential to be active against important Gram-negative pathogens of the Enterobacteriaceae
410 and *P. aeruginosa*. Based on the spectrum of activity vs. Gram-negative pathogens and
411 classes of antibiotics that are potentiated by MBX2319, it could be useful as an adjunctive
412 therapy in combination with a fluoroquinolone, β -lactam, or β -lactam/ β -lactamase inhibitor.

413 **ACKNOWLEDGMENTS.** This paper is dedicated to the memory of our late colleague Chad
414 Houseweart. The research reported in this report was supported by the National Institute of
415 Allergy and Infectious Disease of the National Institutes of Health under award R43AI074116
416 and R43 AI100332. G.C.W. is an American Cancer Society Professor and is supported by NIH
417 grant R01 CA021615. The content is solely the responsibility of the authors and does not
418 necessarily represent the official views of the National Institutes of Health.

LITERATURE CITED

1. **Kang CI, Kim SH, Park WB, Lee KD, Kim HB, Kim EC, Oh MD, Choe KW.** 2005. Risk factors for antimicrobial resistance and influence of resistance on mortality in patients with bloodstream infection caused by *Pseudomonas aeruginosa*. *Microb Drug Resist* **11**:68-74.
2. **Kang CI, Kim SH, Park WB, Lee KD, Kim HB, Kim EC, Oh MD, Choe KW.** 2005. Clinical epidemiology of ciprofloxacin resistance and its relationship to broad-spectrum cephalosporin resistance in bloodstream infections caused by *Enterobacter* species. *Infect Control Hosp Epidemiol* **26**:88-92.
3. **Kang CI, Kim SH, Park WB, Lee KD, Kim HB, Kim EC, Oh MD, Choe KW.** 2005. Bloodstream infections caused by antibiotic-resistant gram-negative bacilli: risk factors for mortality and impact of inappropriate initial antimicrobial therapy on outcome. *Antimicrob Agents Chemother* **49**:760-766.
4. **Kibbey CE, Poole SK, Robinson B, Jackson JD, Durham D.** 2001. An integrated process for measuring the physicochemical properties of drug candidates in a preclinical discovery environment. *J Pharm Sci* **90**:1164-1175.
5. **Peleg AY, Hooper DC.** 2010. Hospital-acquired infections due to gram-negative bacteria. *N Engl J Med* **362**:1804-1813.
6. **Anthony KB, Fishman NO, Linkin DR, Gasink LB, Edelstein PH, Lautenbach E.** 2008. Clinical and microbiological outcomes of serious infections with multidrug-resistant gram-negative organisms treated with tigecycline. *Clin Infect Dis* **46**:567-570.
7. **Nikaido H, Pages JM.** 2012. Broad-specificity efflux pumps and their role in multidrug resistance of Gram-negative bacteria. *FEMS Microbiol Rev* **36**:340-363.
8. **Nikaido H, Takatsuka Y.** 2009. Mechanisms of RND multidrug efflux pumps. *Biochim Biophys Acta* **1794**:769-781.
9. **Piddock LJ.** 2006. Clinically relevant chromosomally encoded multidrug resistance efflux pumps in bacteria. *Clin Microbiol Rev* **19**:382-402.
10. **Li XZ, Zhang L, Srikumar R, Poole K.** 1998. Beta-lactamase inhibitors are substrates for the multidrug efflux pumps of *Pseudomonas aeruginosa*. *Antimicrob Agents Chemother* **42**:399-403.
11. **Nakae T, Saito K, Nakajima A.** 2000. Effect of sulbactam on anti-pseudomonal activity of beta-lactam antibiotics in cells producing various levels of the MexAB-OprM efflux pump and beta-lactamase. *Microbiol Immunol* **44**:997-1001.
12. **Lomovskaya O, Lee A, Hoshino K, Ishida H, Mistry A, Warren MS, Boyer E, Chamberland S, Lee VJ.** 1999. Use of a genetic approach to evaluate the consequences of inhibition of efflux pumps in *Pseudomonas aeruginosa*. *Antimicrob Agents Chemother* **43**:1340-1346.
13. **Lomovskaya O, Warren MS, Lee A, Galazzo J, Fronko R, Lee M, Blais J, Cho D, Chamberland S, Renau T, Leger R, Hecker S, Watkins W, Hoshino K, Ishida H, Lee VJ.** 2001. Identification and characterization of inhibitors of multidrug resistance efflux pumps in *Pseudomonas aeruginosa*: novel agents for combination therapy. *Antimicrob Agents Chemother* **45**:105-116.
14. **Singh R, Swick MC, Ledesma KR, Yang Z, Hu M, Zechiedrich L, Tam VH.** 2012. Temporal interplay between efflux pumps and target mutations in development of antibiotic resistance in *Escherichia coli*. *Antimicrob Agents Chemother* **56**:1680-1685.
15. **Nishino K, Latifi T, Groisman EA.** 2006. Virulence and drug resistance roles of multidrug efflux systems of *Salmonella enterica* serovar Typhimurium. *Mol Microbiol* **59**:126-141.
16. **Kvist M, Hancock V, Klemm P.** 2008. Inactivation of efflux pumps abolishes bacterial biofilm formation. *Appl Environ Microbiol* **74**:7376-7382.

- 466 17. **Van Bambeke F, Pages JM, Lee VJ.** 2006. Inhibitors of bacterial efflux pumps as adjuvants in
467 antibiotic treatments and diagnostic tools for detection of resistance by efflux. *Recent Pat*
468 *Antiinfect Drug Discov* **1**:157-175.
- 469 18. **Renau TE, Leger R, Filonova L, Flamme EM, Wang M, Yen R, Madsen D, Griffith D,**
470 **Chamberland S, Dudley MN, Lee VJ, Lomovskaya O, Watkins WJ, Ohta T, Nakayama K, Ishida Y.**
471 2003. Conformationally-restricted analogues of efflux pump inhibitors that potentiate the
472 activity of levofloxacin in *Pseudomonas aeruginosa*. *Bioorg Med Chem Lett* **13**:2755-2758.
- 473 19. **Renau TE, Leger R, Flamme EM, Sangalang J, She MW, Yen R, Gannon CL, Griffith D,**
474 **Chamberland S, Lomovskaya O, Hecker SJ, Lee VJ, Ohta T, Nakayama K.** 1999. Inhibitors of
475 efflux pumps in *Pseudomonas aeruginosa* potentiate the activity of the fluoroquinolone
476 antibacterial levofloxacin. *J Med Chem* **42**:4928-4931.
- 477 20. **Renau TE, Leger R, Flamme EM, She MW, Gannon CL, Mathias KM, Lomovskaya O,**
478 **Chamberland S, Lee VJ, Ohta T, Nakayama K, Ishida Y.** 2001. Addressing the stability of C-
479 capped dipeptide efflux pump inhibitors that potentiate the activity of levofloxacin in
480 *Pseudomonas aeruginosa*. *Bioorg Med Chem Lett* **11**:663-667.
- 481 21. **Renau TE, Leger R, Yen R, She MW, Flamme EM, Sangalang J, Gannon CL, Chamberland S,**
482 **Lomovskaya O, Lee VJ.** 2002. Peptidomimetics of efflux pump inhibitors potentiate the activity
483 of levofloxacin in *Pseudomonas aeruginosa*. *Bioorg Med Chem Lett* **12**:763-766.
- 484 22. **Watkins WJ, Landaverry Y, Leger R, Litman R, Renau TE, Williams N, Yen R, Zhang JZ,**
485 **Chamberland S, Madsen D, Griffith D, Tembe V, Huie K, Dudley MN.** 2003. The relationship
486 between physicochemical properties, in vitro activity and pharmacokinetic profiles of analogues
487 of diamine-containing efflux pump inhibitors. *Bioorg Med Chem Lett* **13**:4241-4244.
- 488 23. **Lomovskaya O, Bostian KA.** 2006. Practical applications and feasibility of efflux pump inhibitors
489 in the clinic--a vision for applied use. *Biochem Pharmacol* **71**:910-918.
- 490 24. **Nakayama K, Ishida Y, Ohtsuka M, Kawato H, Yoshida K, Yokomizo Y, Hosono S, Ohta T,**
491 **Hoshino K, Ishida H, Yoshida K, Renau TE, Leger R, Zhang JZ, Lee VJ, Watkins WJ.** 2003. MexAB-
492 OprM-specific efflux pump inhibitors in *Pseudomonas aeruginosa*. Part 1: discovery and early
493 strategies for lead optimization. *Bioorg Med Chem Lett* **13**:4201-4204.
- 494 25. **Nakayama K, Ishida Y, Ohtsuka M, Kawato H, Yoshida K, Yokomizo Y, Ohta T, Hoshino K, Otani**
495 **T, Kurosaka Y, Yoshida K, Ishida H, Lee VJ, Renau TE, Watkins WJ.** 2003. MexAB-OprM specific
496 efflux pump inhibitors in *Pseudomonas aeruginosa*. Part 2: achieving activity in vivo through the
497 use of alternative scaffolds. *Bioorg Med Chem Lett* **13**:4205-4208.
- 498 26. **Nakayama K, Kawato H, Watanabe J, Ohtsuka M, Yoshida K, Yokomizo Y, Sakamoto A, Kuru N,**
499 **Ohta T, Hoshino K, Yoshida K, Ishida H, Cho A, Palme MH, Zhang JZ, Lee VJ, Watkins WJ.** 2004.
500 MexAB-OprM specific efflux pump inhibitors in *Pseudomonas aeruginosa*. Part 3: Optimization
501 of potency in the pyridopyrimidine series through the application of a pharmacophore model.
502 *Bioorg Med Chem Lett* **14**:475-479.
- 503 27. **Nakayama K, Kuru N, Ohtsuka M, Yokomizo Y, Sakamoto A, Kawato H, Yoshida K, Ohta T,**
504 **Hoshino K, Akimoto K, Itoh J, Ishida H, Cho A, Palme MH, Zhang JZ, Lee VJ, Watkins WJ.** 2004.
505 MexAB-OprM specific efflux pump inhibitors in *Pseudomonas aeruginosa*. Part 4: Addressing the
506 problem of poor stability due to photoisomerization of an acrylic acid moiety. *Bioorg Med Chem*
507 *Lett* **14**:2493-2497.
- 508 28. **Yoshida K, Nakayama K, Kuru N, Kobayashi S, Ohtsuka M, Takemura M, Hoshino K, Kanda H,**
509 **Zhang JZ, Lee VJ, Watkins WJ.** 2006. MexAB-OprM specific efflux pump inhibitors in
510 *Pseudomonas aeruginosa*. Part 5: Carbon-substituted analogues at the C-2 position. *Bioorg Med*
511 *Chem* **14**:1993-2004.
- 512 29. **Yoshida K, Nakayama K, Ohtsuka M, Kuru N, Yokomizo Y, Sakamoto A, Takemura M, Hoshino**
513 **K, Kanda H, Nitanai H, Namba K, Yoshida K, Imamura Y, Zhang JZ, Lee VJ, Watkins WJ.** 2007.

- MexAB-OprM specific efflux pump inhibitors in *Pseudomonas aeruginosa*. Part 7: highly soluble and in vivo active quaternary ammonium analogue D13-9001, a potential preclinical candidate. *Bioorg Med Chem* **15**:7087-7097.
30. **Yoshida K, Nakayama K, Yokomizo Y, Ohtsuka M, Takemura M, Hoshino K, Kanda H, Namba K, Nitani H, Zhang JZ, Lee VJ, Watkins WJ.** 2006. MexAB-OprM specific efflux pump inhibitors in *Pseudomonas aeruginosa*. Part 6: exploration of aromatic substituents. *Bioorg Med Chem* **14**:8506-8518.
31. **Baba T, Ara T, Hasegawa M, Takai Y, Okumura Y, Baba M, Datsenko KA, Tomita M, Wanner BL, Mori H.** 2006. Construction of *Escherichia coli* K-12 in-frame, single-gene knockout mutants: the Keio collection. *Mol Syst Biol* **2**:2006 0008.
32. **CLSI.** 2006. Method for dilution antimicrobial susceptibility testing for bacteria that grow aerobically; Approved standard-document M7-A7. Clinical and Laboratory Standards Institute, Wayne, PA.
33. **Pillai SK, Moellering RC, Eliopoulos GM.** 2005. Antimicrobial Combinations, p. 365-440. *In* Lorian V (ed.), *Antibiotics in Laboratory Medicine*, 5th ed. Lippincott Williams & Wilkins, Philadelphia, PA.
34. **Coldham NG, Webber M, Woodward MJ, Piddock LJ.** 2010. A 96-well plate fluorescence assay for assessment of cellular permeability and active efflux in *Salmonella enterica* serovar Typhimurium and *Escherichia coli*. *J Antimicrob Chemother* **65**:1655-1663.
35. **Nagano K, Nikaido H.** 2009. Kinetic behavior of the major multidrug efflux pump AcrB of *Escherichia coli*. *Proc Natl Acad Sci U S A* **106**:5854-5858.
36. **Bohnert JA, Karamian B, Nikaido H.** 2010. Optimized Nile Red efflux assay of AcrAB-TolC multidrug efflux system shows competition between substrates. *Antimicrob Agents Chemother* **54**:3770-3775.
37. **Butler MM, Lamarr WA, Foster KA, Barnes MH, Skow DJ, Lyden PT, Kustigian LM, Zhi C, Brown NC, Wright GE, Bowlin TL.** 2007. Antibacterial activity and mechanism of action of a novel anilino-uracil-fluoroquinolone hybrid compound. *Antimicrob Agents Chemother* **51**:119-127.
38. **Schumacher A, Steinke P, Bohnert JA, Akova M, Jonas D, Kern WV.** 2006. Effect of 1-(1-naphthylmethyl)-piperazine, a novel putative efflux pump inhibitor, on antimicrobial drug susceptibility in clinical isolates of Enterobacteriaceae other than *Escherichia coli*. *J Antimicrob Chemother* **57**:344-348.
39. **Okusu H, Ma D, Nikaido H.** 1996. AcrAB efflux pump plays a major role in the antibiotic resistance phenotype of *Escherichia coli* multiple-antibiotic-resistance (Mar) mutants. *J Bacteriol* **178**:306-308.
40. **Ma D, Alberti M, Lynch C, Nikaido H, Hearst JE.** 1996. The local repressor AcrR plays a modulating role in the regulation of *acrAB* genes of *Escherichia coli* by global stress signals. *Mol Microbiol* **19**:101-112.
41. **Zgurskaya HI, Nikaido H.** 1999. Bypassing the periplasm: reconstitution of the AcrAB multidrug efflux pump of *Escherichia coli*. *Proc Natl Acad Sci U S A* **96**:7190-7195.
42. **Patel L, Garcia ML, Kaback HR.** 1982. Direct measurement of lactose/proton symport in *Escherichia coli* membrane vesicles: further evidence for the involvement of histidine residue(s). *Biochemistry* **21**:5805-5810.
43. **Eicher T, Cha HJ, Seeger MA, Brandstatter L, El-Delik J, Bohnert JA, Kern WV, Verrey F, Grutter MG, Diederichs K, Pos KM.** 2012. Transport of drugs by the multidrug transporter AcrB involves an access and a deep binding pocket that are separated by a switch-loop. *Proc Natl Acad Sci U S A* **109**:5687-5692.
44. **Murakami S, Nakashima R, Yamashita E, Matsumoto T, Yamaguchi A.** 2006. Crystal structures of a multidrug transporter reveal a functionally rotating mechanism. *Nature* **443**:173-179.

- 562 45. **Takatsuka Y, Chen C, Nikaido H.** 2010. Mechanism of recognition of compounds of diverse
563 structures by the multidrug efflux pump AcrB of *Escherichia coli*. *Proc Natl Acad Sci U S A*
564 **107**:6559-6565.
- 565 46. **Vargiu AV, Nikaido H.** 2012. Multidrug binding properties of the AcrB efflux pump characterized
566 by molecular dynamics simulations. *Proc Natl Acad Sci U S A* **109**:20637-20642.
- 567 47. **Nakashima R, Sakurai K, Yamasaki S, Nishino K, Yamaguchi A.** 2011. Structures of the multidrug
568 exporter AcrB reveal a proximal multisite drug-binding pocket. *Nature* **480**:565-569.
- 569 48. **Pages JM, Amaral L.** 2009. Mechanisms of drug efflux and strategies to combat them:
570 challenging the efflux pump of Gram-negative bacteria. *Biochim Biophys Acta* **1794**:826-833.
- 571 49. **Sennhauser G, Bukowska MA, Briand C, Grutter MG.** 2009. Crystal structure of the multidrug
572 exporter MexB from *Pseudomonas aeruginosa*. *J Mol Biol* **389**:134-145.
- 573 50. **Tikhonova EB, Wang Q, Zgurskaya HI.** 2002. Chimeric analysis of the multicomponent multidrug
574 efflux transporters from gram-negative bacteria. *J Bacteriol* **184**:6499-6507.
- 575 51. **Dewitt SK, Adelberg EA.** 1962. The Occurrence of a Genetic Transposition in a Strain of
576 *Escherichia Coli*. *Genetics* **47**:577-585.
- 577 52. **Holloway BW.** 1955. Genetic recombination in *Pseudomonas aeruginosa*. *J Gen Microbiol*
578 **13**:572-581.

585 **Table 1.** Bacterial strains that were used in this study.

Organism	Strain	Genotype/Description	Source (Ref)
<i>Escherichia coli</i>	AB1157	<i>thr-1, araC14, leuB6</i> (Am), Δ (<i>gpt-proA</i>)62, <i>lacY1, tsx-33, qsr'-0, glnV44</i> (AS), <i>galK2</i> (Oc), LAM-, Rac-0, <i>hisG4</i> (Oc), <i>rfbC1, mgl-51, rpoS396</i> (Am), <i>rpsL31</i> (strR), <i>kdgK51, xylA5, mtl-1, argE3</i> (Oc), <i>thi-1</i>	(51)
<i>Escherichia coli</i>	Δ <i>tolC</i>	AB1157, Δ <i>tolC</i> ::kan	this study
<i>Escherichia coli</i>	Δ <i>acrB</i>	AB1157, Δ <i>acrB</i> ::kan	this study
<i>Escherichia coli</i>	Δ <i>acrF</i>	AB1157, Δ <i>acrF</i> ::kan	this study
<i>Escherichia coli</i>	Δ <i>macB</i>	AB1157, Δ <i>macB</i> ::kan	this study
<i>Escherichia coli</i>	Δ <i>emrB</i>	AB1157, Δ <i>emrB</i> ::kan	this study
<i>Escherichia coli</i>	285	AB1157, CIP ^R , Overexpresses efflux*	this study
<i>Escherichia coli</i>	287	AB1157, CIP ^R , Overexpresses efflux*	this study
<i>Escherichia coli</i>	331	CIP ^R , UTI isolate	Baylor College of Medicine
<i>Escherichia coli</i>	ATCC 25922		ATCC#
<i>Escherichia coli</i>	HN1157	F', <i>araD139, \Delta</i> (<i>argF-lac</i>)U169, <i>rpsL150, rel-I, flb-5301, ptsF25, deoCI, thi-J, \Delta</i> <i>lamB106, \Delta</i> <i>ompF80, zeio6</i> ::Tn10, <i>ompCI24, acrR</i> ::kan	(35)
<i>Escherichia coli</i>	HN1159	HN1157, Δ <i>acrAB</i> :: <i>spc</i>	(35)
<i>Enterobacter cloacae</i>	ATCC 13047		ATCC#
<i>Enterobacter aerogenes</i>	ATCC 13048		ATCC#
<i>Klebsiella pneumoniae</i>	ATCC 700603		ATCC#
<i>Klebsiella pneumoniae</i>	ATCC 13882		ATCC#
<i>Shigella flexneri</i>	ATCC 12022		ATCC#
<i>Salmonella enterica</i> (typhimurium)	ATCC 14028		ATCC#
<i>Pseudomonas aeruginosa</i>	PA01		(52)
<i>Pseudomonas aeruginosa</i>	ATCC 27853		ATCC#
<i>Proteus mirabilis</i>	ATCC 25933		ATCC#
<i>Proteus mirabilis</i>	BAA-856	UTI clinical isolate	ATCC#

#ATCC, American Type Culture Collection

*isolated as a ciprofloxacin resistant mutant during a serial passage in subinhibitory levels of ciprofloxacin

586
587
588

Table 2. MBX2319 potentiates the antibacterial activity of fluoroquinolone and β -lactam antibiotics against *E. coli* strains that are efflux proficient and efflux over-expressers (EOE), but not against $\Delta acrB$ or $\Delta tolC$ mutants.

Strain	MIC (μ M)	Drug	MIC (μ g/ml) with MBX2319 at concn (μ M) of:							MIC ratios	
	MBX2319		0	1.56	3.13	6.25	12.5	25	50	2319 ^a	mutant ^b
AB1157 (WT)	≥ 100	CIP	0.016	0.008	0.008	0.008	0.008	0.008	0.008	2	1
		LEV	0.063	0.031	0.016	0.016	0.016	0.016	0.016	4	1
		PIP	4	2	1	1	0.5	0.5	0.5	8	1
$\Delta tolC$	≥ 100	CIP	0.004	0.004	0.004	0.004	0.004	0.004	0.004	1	4
		LEV	0.016	0.016	0.016	0.008	0.008	0.008	0.008	2	4
		PIP	0.125	0.125	0.125	0.125	0.125	0.125	0.125	1	32
$\Delta acrB$	≥ 100	CIP	0.004	0.004	0.004	0.004	0.004	0.004	0.004	1	4
		LEV	0.016	0.016	0.016	0.016	0.016	0.016	0.016	1	4
		PIP	0.250	0.125	0.125	0.125	0.125	0.125	0.125	2	16
$\Delta acrF$	≥ 100	CIP	0.016	0.008	0.008	0.008	0.008	0.008	0.008	2	1
		LEV	0.063	0.031	0.031	0.016	0.016	0.016	0.016	4	1
		PIP	4	2	1	0.5	0.5	0.5	0.5	8	1
285 (EOE)	≥ 100	CIP	1	0.25	0.125	0.125	0.125	0.125	0.125	8	0.016
		LEV	2	0.5	0.25	0.25	0.25	0.25	0.25	8	0.031
		PIP	8	4	2	2	2	2	2	4	0.5
		CEF	0.25	0.125	0.063	0.063	0.063	0.031	0.031	8	0.25
285 $\Delta tolC$	≥ 100	CIP	0.063	0.063	0.063	0.063	0.063	0.063	0.063	1	0.25
		LEV	0.063	0.063	0.063	0.063	0.063	0.063	0.063	1	1
		PIP	0.25	0.25	0.25	0.25	0.25	0.25	0.25	1	16
		CEF	0.031	0.031	0.031	0.031	0.031	0.031	0.031	1	2
287 (EOE)	≥ 100	CIP	1	0.5	0.25	0.25	0.25	0.25	0.25	4	0.016
		LEV	2	0.5	0.5	0.5	0.5	0.25	0.25	8	0.031
		PIP	16	8	4	4	2	2	2	8	0.25
		CEF	0.25	0.125	0.125	0.063	0.063	0.063	0.063	4	0.25
287 $\Delta tolC$	≥ 100	CIP	0.125	0.125	0.125	0.125	0.125	0.125	0.125	1	0.125
		LEV	0.125	0.125	0.125	0.125	0.125	0.125	0.125	1	0.5
		PIP	0.25	0.25	0.25	0.25	0.25	0.25	0.25	1	16
		CEF	0.015	0.015	0.015	0.015	0.015	0.015	0.015	1	4

^a: highest ratio of MIC (no compound) / MIC (MBX2319)

^b: MIC (WT) / MIC (mutant) in the absence of EPI

Abbreviations: EOE, Efflux Over-Expresser; CIP, ciprofloxacin; LEV, levofloxacin; PIP, piperacillin; CEF, cefotaxime.

Table 3. MBX2319 potentiates the antibacterial activity of diverse antibacterial agents and biocides.

Cmpd	MICs* (µg/ml) ± EPIs‡					MIC Ratio			
	WT			Δ <i>acrB</i>	Δ <i>tolC</i>				
	None	2319	PAβN	None	None	2319 ^a	PAβN ^b	Δ <i>acrB</i> ^c	Δ <i>tolC</i> ^d
CIP	0.016	0.008	0.031	0.008	0.004	2	0.5	2	4
LEV	0.063	0.016	0.031	0.016	0.016	4	2	4	4
NOR	0.063	0.031	0.125	0.031	0.031	2	0.5	2	2
NAL	16	4	2	2	1	4	8	8	16
PIP	4	0.5	8	0.25	0.25	8	0.5	16	16
CLX	512	64	256	4	1	8	2	128	512
OXA	512	64	128	4	1	8	4	128	512
CAR	4	8	16	2	1	0.5	0.25	2	4
CM	8	2	2	2	1	4	4	4	8
TET	2	1	2	0.5	0.5	2	1	4	4
GM	8	8	4	8	4	1	2	1	2
RIF	16	8	4	8	8	2	4	2	2
NOV	128	128	128	16	2	1	1	8	64
ERM	128	16	4	2	2	8	32	64	64
LIN	240	60	120	15	15	4	2	16	16
EtBr	256	256	256	32	8	1	1	8	32
CV	32	8	8	1	1	4	4	32	32
IRG	0.5	0.25	0.25	0.125	0.016	2	2	4	32
ACR	32	32	32	4	4	1	1	8	8
CHX	1	1	1	1	1	1	1	1	1
BAC	32	16	8	2	2	2	4	16	16
CPC	4	4	2	2	2	1	2	2	2

*, Geometric mean of MICs from at least three replicate experiments. ‡, The final concentration of the EPIs MBX2319 and PAβN was 25 µM. ^a, MIC no cmpd / MIC +25 µM MBX2319; ^b, MIC no cmpd / MIC +25 µM PAβN; ^c, MIC WT/ MIC Δ*acrB*; ^d, MIC WT/ MIC Δ*tolC*.

Abbreviations: 2319, MBX2319; CIP, ciprofloxacin; LEV, levofloxacin; NOR, norfloxacin; NAL, nalidixic acid; PIP, piperacillin; CLX, cloxacillin; OXA, oxacillin; CAR, carbenicillin; CM, chloramphenicol; TET, tetracycline; GM, gentamicin; RIF, rifampicin; NOV, novobiocin; ERM, erythromycin; LIN, linezolid; EtBr, ethidium bromide; CV, crystal violet; IRG, irgasan (triclosan); ACR, acriflavine; CHX, chlorhexidine; BAC, benzalkonium chloride; CPC, cetylpyridinium chloride.

Table 4. TMG accumulation in *E. coli* HN1157 in the presence of MBX2319.

Compound	Conc. (μ M)	N	TMG accumulation (nmole/mg dry wt) (Mean \pm SD)	Percent Control
None	0	9	10.7 \pm 1.5	100
CCCP	100	9	0.3 \pm 0.1	3
MBX2319	0.2	3	10.5 \pm 1.8	98
MBX2319	2	3	11.7 \pm 0.9	109
MBX2319	20*	3	9.9 \pm 0.3	92

*compound was slightly above the solubility limit in assay buffer

620 **Table 5.** Spectrum of activity of MBX2319.

Organism	Drug	MIC* (µg/ml) ± EPI‡			MIC ratio	
		None	MBX2319	PAβN	MBX2319 ^a	PAβN ^b
<i>Escherichia coli</i> AB1157	CIP	0.016	0.008	0.031	2	0.5
	LEV	0.031	0.016	0.031	2	1
	PIP	4	0.707	4	5.7	1
	CEF	0.1	0.022	0.25	4.8	0.42
<i>Escherichia coli</i> ATCC 25922	CIP	0.016	0.005	0.022	2.8	0.7
	LEV	0.031	0.013	0.022	2.4	1.4
	PIP	2.83	1.68	4	1.7	0.7
	CEF	0.074	0.063	0.25	1.2	0.3
<i>Escherichia coli</i> 331	CIP	128	32	128	4	1
	LEV	64	11.3	32	5.6	2
	PIP	4	0.707	4	5.6	1
	CEF	0.125	0.031	0.353	4	0.353
<i>Salmonella enterica</i> ATCC 14028	CIP	0.031	0.008	0.044	4	0.7
	LEV	0.062	0.016	0.044	4	1.4
	PIP	2.4	0.5	4	4.8	0.6
	CEF	0.21	0.063	0.297	3.4	0.7
<i>Shigella flexneri</i> ATCC 12022	CIP	0.031	0.008	0.031	4	1
	LEV	0.063	0.016	0.031	4	2
	PIP	1	0.25	1	4	1
	CEF	0.063	0.031	0.063	2	1
<i>Enterobacter aerogenes</i> ATCC 13048	CIP	0.037	0.008	0.031	4.8	1.2
	LEV	0.177	0.044	0.063	4	2.8
	PIP	4	1.4	16	2.8	0.2
	CEF	2	2.4	6.7	0.8	0.3
<i>Klebsiella pneumoniae</i> ATCC 700603	CIP	0.29	0.088	0.25	3.4	1.2
	LEV	0.71	0.149	0.5	4.7	1.4
	PIP	113	113	113	1	1
	CEF	8	8	8	1	1
<i>P. aeruginosa</i> PA01	CIP	0.22	0.28	0.14	0.8	1.6
	LEV	1.6	2	0.89	0.8	1.8
	PIP	4	2	4	2	1
	CEF	8	4	8	2	1
<i>P. aeruginosa</i> ATCC 27853	CIP	0.21	0.125	0.149	1.7	1.4
	LEV	1	1	0.5	1	2
	PIP	16	19	19	0.84	0.8
	CEF	53.8	8	19	6.7	2.8

621 *: Geometric mean of MICs from at least three replicate experiments. ‡: The final concentration of the EPIs
622 MBX2319 and PAβN was 25 µM. ^a: MIC no compd / MIC +25 µM MBX2319. ^b: MIC no compd / MIC +25 µM PAβN.
623 Abbreviations: CIP, ciprofloxacin; LEV, levofloxacin; PIP, piperacillin; CEF, cefotaxime.

Figure 1. Structures of the efflux pump inhibitors MBX2319 and PA β N.

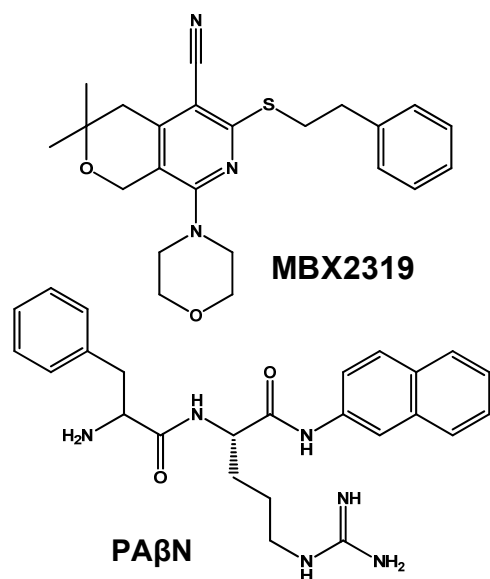


Figure 2. The effects of the efflux pump inhibitors MBX2319 and PA β N on the bactericidal activity of ciprofloxacin (CIP) in time-kill assays. **A)** Bactericidal activity of varying concentrations of MBX2319 (0.19-3.13 μ M) combined with a bacteristatic concentration of CIP (1 \times MIC, 0.01 μ g/ml) against *E. coli* AB1157. **B)** Bactericidal activity of varying concentrations of PA β N (6.25-100 μ M) combined with a minimally bactericidal concentration of CIP (1 \times MIC, 0.01 μ g/ml) against *E. coli* AB1157. **C)** Bactericidal activity of 25 μ M MBX2319 combined with a minimally bactericidal concentration of CIP against *E. coli* AB1157 and isogenic efflux defective mutants after 2 h exposure. Dark bars, CIP alone (1 \times MIC, 0.01 μ g/ml); Light bars CIP + 25 μ M MBX2319. **D)** Bactericidal activity of 25 μ M MBX2319 combined with a minimally bactericidal concentration of CIP against the following organisms: **a)** *E. coli* AB1157, **b)** *E. coli* ATCC 25922, **c)** *K. pneumoniae* ATCC 700603, **d)** *S. flexneri* ATCC 12022, **e)** *S. enterica* ATCC 14028, **f)** *E. aerogenes* ATCC 13048.

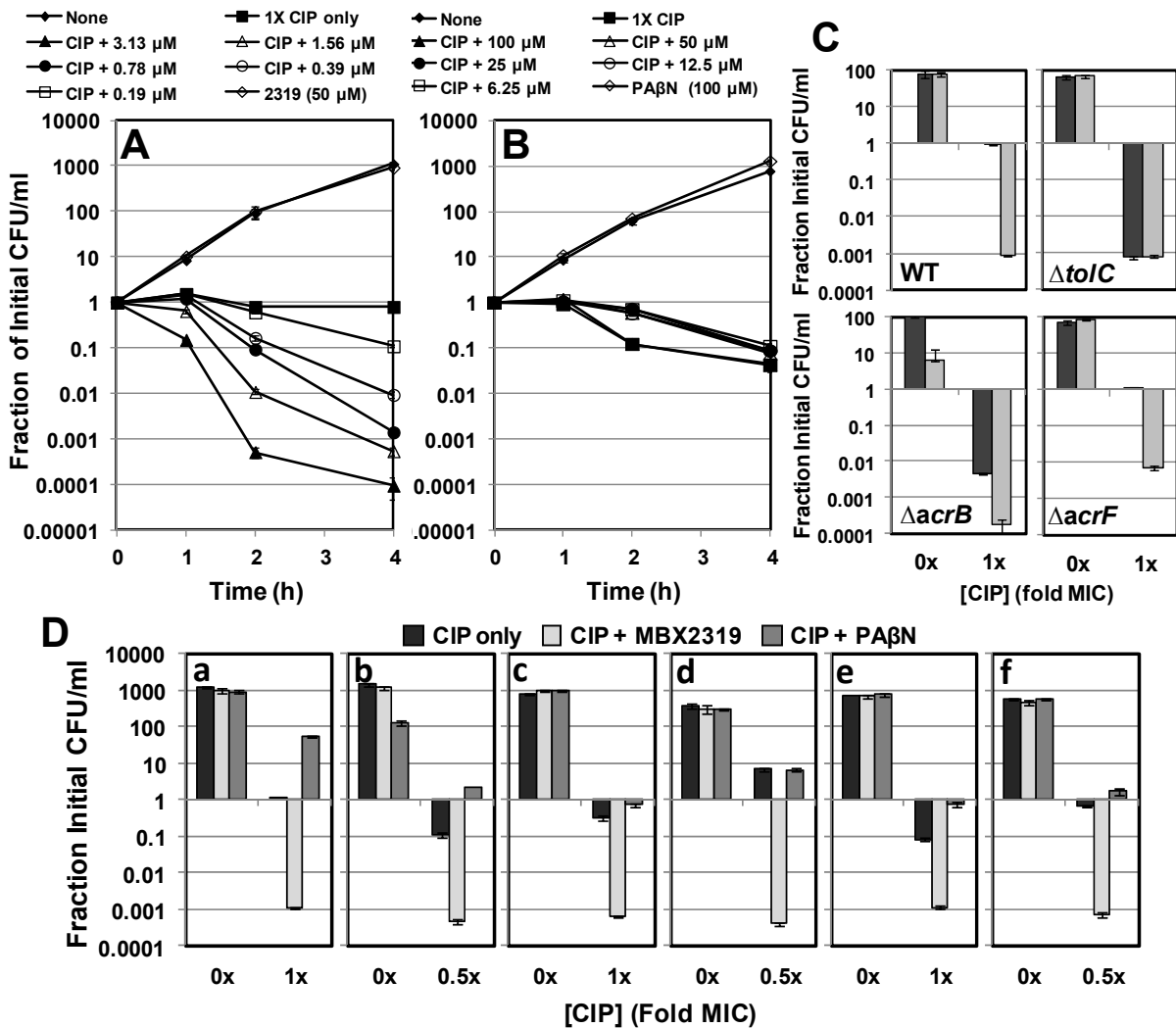


Figure 3. The effects of MBX2319 and PA β N on the accumulation of the fluorescent DNA-binding dye H33342, an AcrAB efflux pump substrate, in *E. coli* AB1157. **A)** MBX2319, **B)** PA β N. **C)** The effect of MBX2319 in H33342 accumulation in *E. coli* AB1157 and isogenic efflux-defective mutants. **D)** The effect of MBX2319 in H33342 accumulation in *E. coli* AB1157 and isogenic mutants 285 and 287, which exhibit reduced susceptibility to Ciprofloxacin due to overexpression of efflux pumps.

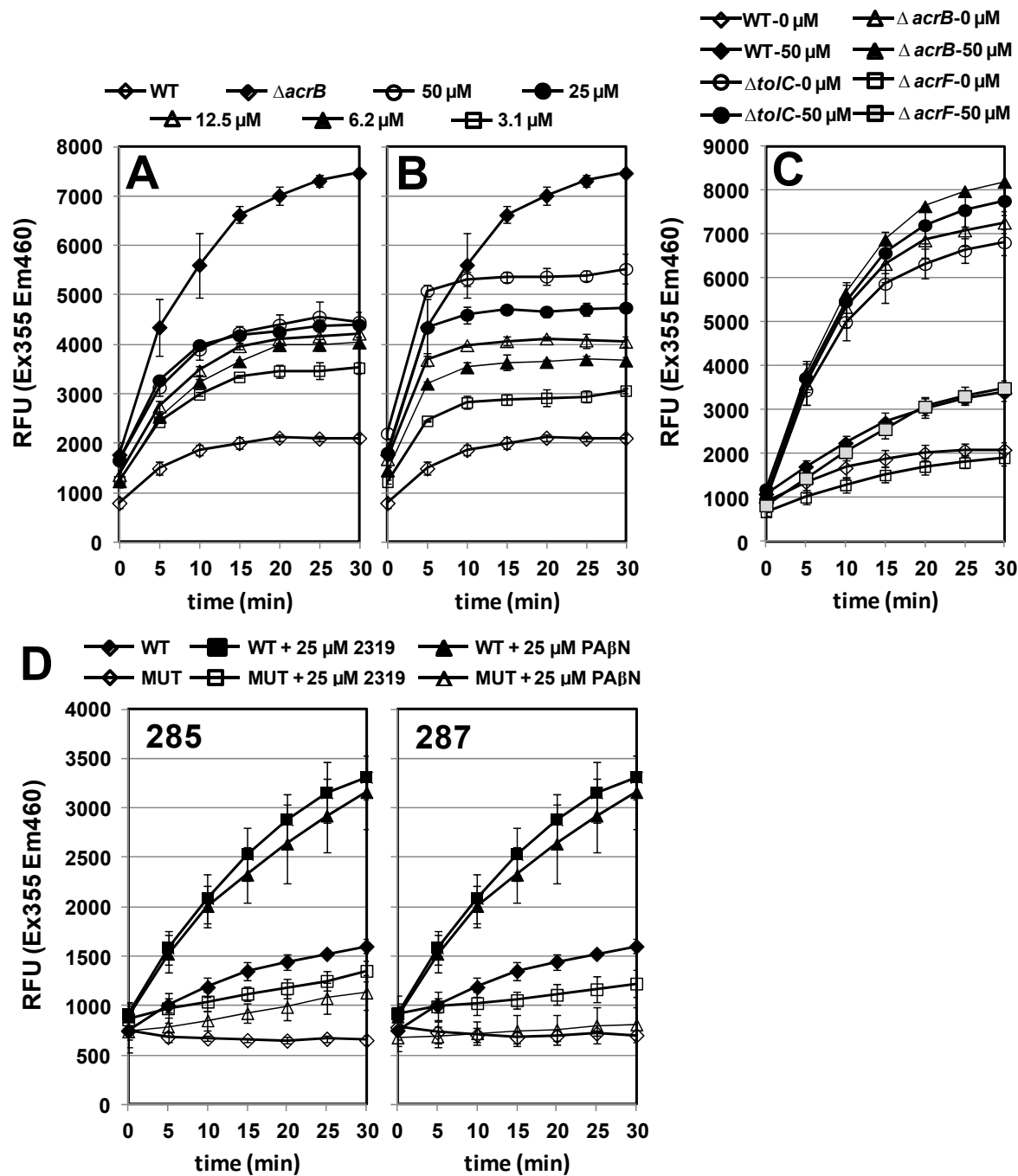


Figure 4. The effects of MBX2319 and PAβN on the kinetic parameters (K_m and V_{max}) of the AcrAB-TolC efflux pump in intact *E. coli* HN1157 cells using the nitrocefin efflux assay. **A)** *E. coli* HN1157 cells treated with 0.2 μM MBX2319, **B)** *E. coli* HN1157 cells treated with 1 μM PAβN.

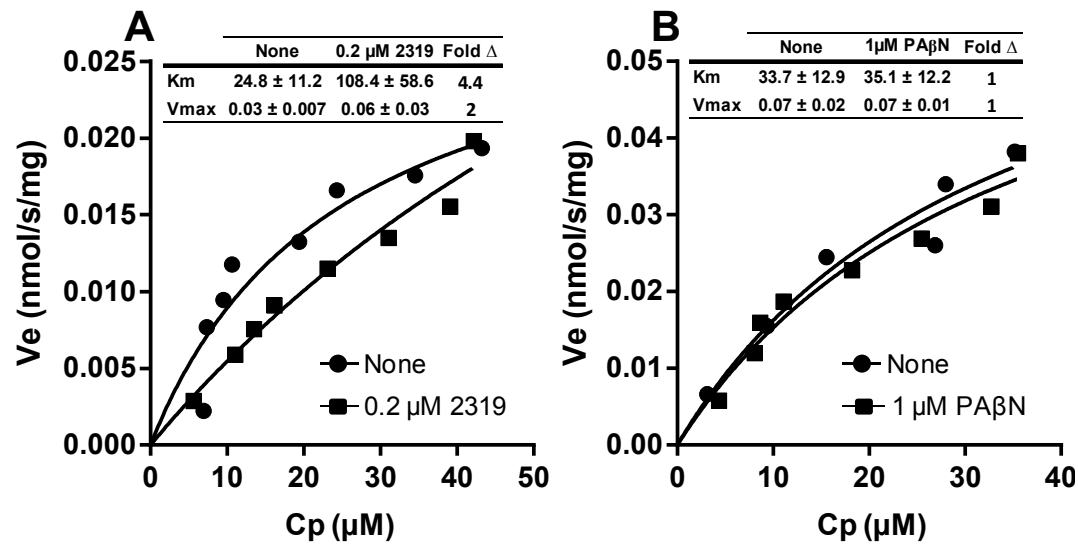


Figure 5. . The effects of MBX2319 and PAβN on the accumulation of H33342 in various Gram-negative organisms. **A)** *E. coli* AB1157, **B)** *E. coli* 331, **C)** *Shigella flexneri* ATCC 12022, **D)** *Klebsiella pneumoniae* ATCC 13882, **E)** *Salmonella enterica* (typhimurium) ATCC 14028, **F)** *Enterobacter cloacae* subsp. *cloacae* ATCC 13047, **G)** *Proteus mirabilis* ATCC 25933, **H)** *Pseudomonas. aeruginosa* ATCC 27835.

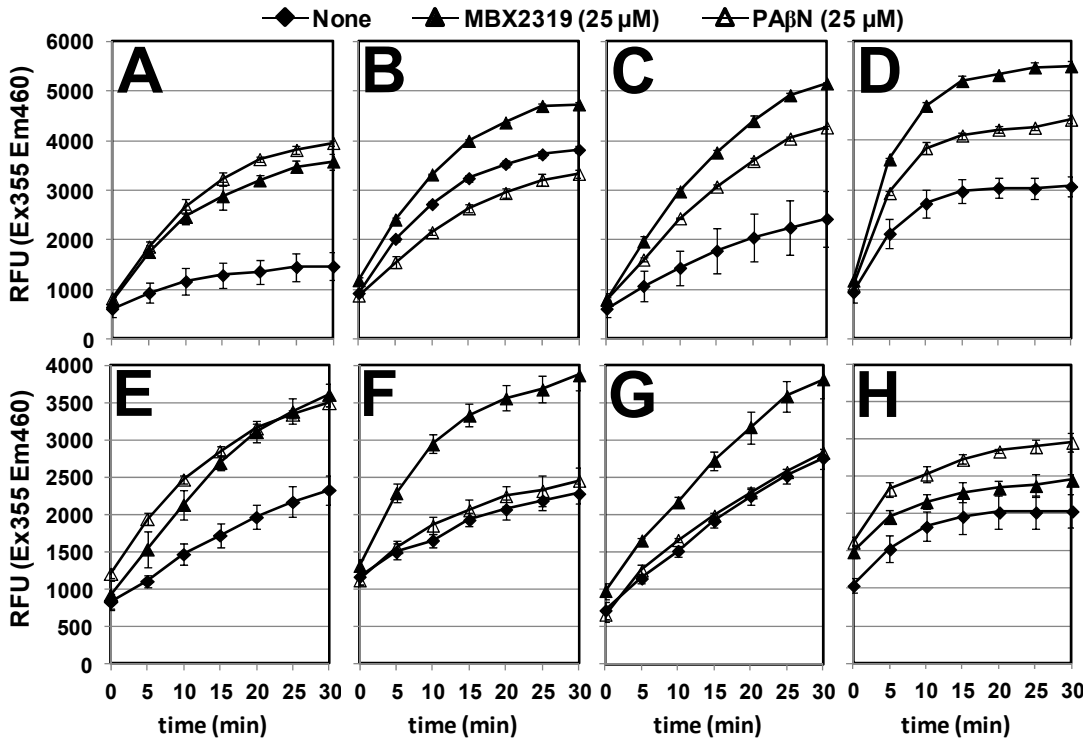
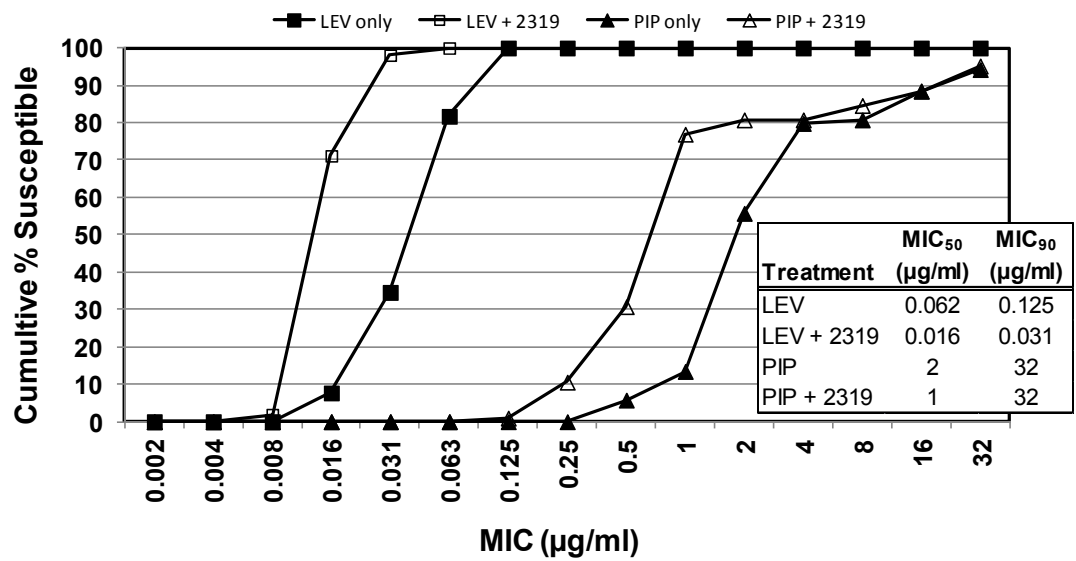


Figure 6. Cumulative MICs for levofloxacin and piperacillin against a panel of 25 strains of *E. coli* strains in the absence and presence of 25 μ M MBX2319.



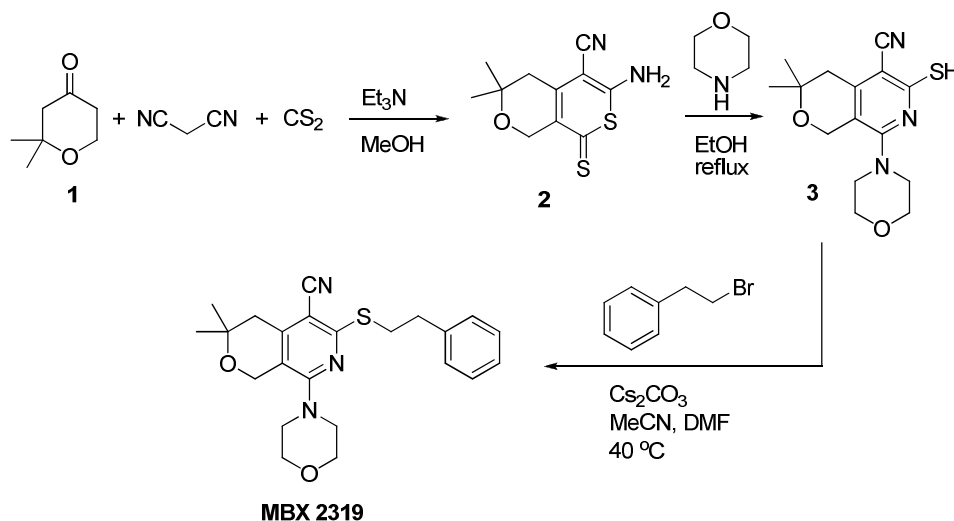
Supplemental Material

Synthesis of MBX 2319. All commercially obtained solvents and reagents were used as received. ^1H NMR spectra were recorded on a Bruker 300 MHz instrument. Chemical shifts are given in δ values referenced to the internal standard tetramethylsilane. MS spectra were recorded on a Thermo LCQ Fleet instrument.

6-amino-5-cyano-3,3-dimethyl-8-thioxo-1,3,4,8-tetrahydrothiopyrano[3,4-*c*]pyran (2) (1, 2). To a stirred solution of 2,2-dimethyltetrahydropyran-4-one (**1**) (3.2 g, 25 mmol), was added portion-wise malononitrile (1.65 g, 25 mmol), followed by carbon disulfide (3 mL, 50 mmol) in methanol (8 mL), and triethylamine (1.5 mL). After stirring at rt overnight, the orange-colored suspension was filtered. The solid was rinsed with diethyl ether (5 mL) to provide compound **2** (2.7 g, 43% yield). R_f : 0.54 (EtOAc: hexanes, 1:1), [UV]; ^1H NMR (DMSO- d_6) δ : 1.19 (s, 6H), 2.57 (s, 2H), 4.46 (s, 2H), 8.91 (br s, 2H); MS (ES+ve) 253.0 (MH $^+$).

6-mercapto-5-cyano-3,3-dimethyl-8-morpholino-3,4-dihydro-1H-pyrano[3,4-*c*]pyridine (3) (1, 2). Morpholine (21.6 mL, 250 mmol) was added to a stirred suspension of compound **2** (2.1 g, 8.32 mmol) in ethanol (30 mL). Reaction mixture was refluxed under nitrogen overnight. After cooling to rt, the mixture was left in an ice bath for 3h and filtered. The solid was rinsed with cold ethanol (3 mL x 2), and dried to provide compound **3** (1.6 g, 63% yield). R_f : 0.49 (EtOAc), [UV]; ^1H NMR (CDCl $_3$) δ : 4.53 (s, 2H), 3.80 (t, 3H), 3.68 (t, 1H), 3.30-3.24 (m, 4H), 2.79 (s, 0.5H), 2.76 (s, 1.5H), 1.33 (s, 6H); MS (ES+ve) 307.0 (MH $^+$).

3,3-dimethyl-5-cyano-8-morpholino-6-(phenethylthio)-3,4-dihydro-1H-pyrano[3,4-*c*]pyridine (MBX 2319). To a stirred solution of compound **3** (1 g, 3.27 mmol) in acetonitrile (12 mL) and DMF (3 mL) was added cesium carbonate (2 g, 6.54 mmol), followed by 2-bromoethyl benzene (910 mg, 4.9 mmol). The solution was heated overnight to 40 °C. The mixture was allowed to cool to rt, water (50 mL) was added. Product was extracted with EtOAc (3 x 50 mL). The combined organic extracts were washed with brine, dried over Na $_2$ SO $_4$ and concentrated by rotary evaporation. The residue was purified by silica gel column chromatography (80 g of SiO $_2$, eluent MeOH: CH $_2$ Cl $_2$, 90: 10, v/v) to provide **MBX 2319** (1.08g, 80% yield) as white powder. R_f : 0.54 (1:1 EtOAc: hexanes), [UV]; ^1H NMR (DMSO- d_6) δ : 1.25 (s, 6H), 2.68 (m, 2H), 2.97 (m, 2H), 3.31 (m, 4H), 3.43 (m, 2H), 3.68 (m, 4H), 4.49 (s, 2H), 7.23-7.30 (m, 5H); MS (ES+ve) 410.0 (MH $^+$).



Scheme 1. Synthesis of MBX2319.

Selection of *E. coli* 285 and 287. Mutants of *E. coli* AB1157 with reduced susceptibility to CIP were selected in a serial passage experiment as follows. Eight independent populations of *E. coli* AB1157 (populations A-H) were grown in 96 well assay plates in LB at 37 °C in the presence of several concentrations of CIP (0.125× - 128× MIC). On day 1 of the experiment, each well of the assay plate was inoculated with approximately 1×10^4 CFU of exponentially growing parent strain. After 16-18 h growth, 50 µl culture was recovered from the wells with highest compound concentration that exhibited robust growth (>50% of untreated control) for each population, were diluted 1:1000 in fresh LB, and were used to inoculate the assay plate containing CIP (0.125× - 128× MIC) for the next culture. This process was repeated for 20 days. The assay plates from each serial passage were stored at -80 °C after the addition of glycerol to each well at a final concentration of 20%. All populations exhibited decreased susceptibility to CIP. Several colonies were isolated and purified from the frozen resistant cultures of day 20 of the serial passage. Decreased susceptibility to CIP and LEV of the purified resistant mutants was confirmed using MIC assays. The resistant clones were added to the strain collection at Microbiotix and were given strain numbers. Based on the MIC data, *E. coli* strains 285 and 287 were chosen for further analyses.

Characterization of *E. coli* 285 and 287.

*Reduced susceptibility to FQs of *E. coli* 285 and 287 is efflux dependent.* The MIC data presented in Table S1 demonstrate that the MICs for CIP and LEV against *E. coli* 285 and 287 are 128–256 and 32-64 -fold higher than AB1157 (WT), respectively. Several important efflux pumps in *E. coli*, such as AcrAB, AcrEF, AcrAD, EmrAB, and MacAB, require the TolC protein for activity [REF]. Therefore, we can assess the role of efflux in the decreased susceptibility to CIP and LEV of *E. coli* 285 and 287 by measuring the MICs of isogenic TolC deficient strains. The $\Delta tolC::kan$ mutation was introduced into *E. coli* 285 and 287 by P1vir transduction, and the MICs for CIP and LEV were determined. The data, shown in Table S1, demonstrate that the MICs for CIP against the $\Delta tolC$ mutants were only 8-16 fold higher than AB1157, indicating that efflux plays a major role in reduced susceptibility to CIP. Likewise, the MICs for LEV against the $\Delta tolC$ mutants were the same as those for AB1157, indicating that efflux is solely responsible for decreased susceptibility to LEV.

**E. coli* 285 and 287 are resistant to diverse antibacterial agents.* Overexpression of one or more efflux pumps is expected to result in decreased susceptibility to several structurally diverse antimicrobial agents. To verify that *E. coli* 285 and 287 overexpress one or more efflux pumps, we determined the MICs for a diverse panel of antimicrobial agents. *E. coli* 285 and 287 exhibited elevated MICs for the β -lactam antibiotics piperacillin (PIP) and cefotaxime (CEF), tetracycline, and chloramphenicol (see Table S2), which are known substrates of AcrAB-TolC. However, *E. coli* 285 and 287 did not exhibit reduced susceptibility to gentamicin, which is not an AcrAB-TolC substrate.

H33342 Accumulation Assay. The H33342 accumulation assay was performed as described in Methods and Materials, except *E. coli* AB1157 (WT), 285, and 287 were exposed to concentrations of H33342 ranging from 2.5-10 µM. The data is shown in Fig. S1. The WT and mutant strains exhibited dose dependent increases in H33342 accumulation over the course of the assay. However, H33342 accumulation in 285 and 287 was significantly lower than WT at all concentrations tested. These results indicate that the efflux activity of 285 and 287 is significantly higher than WT, probably due to over-expression of one or more efflux pumps.

Table S1. Increased efflux activity makes a significant contribution to the decreased susceptibility to fluoroquinolones Ciprofloxacin (CIP) and Levofloxacin (LEV) in *E. coli* 285 and 287. The $\Delta tolC::kan$ mutation, which affects multiple efflux pumps, was introduced into *E. coli* 285 and 287, and the MICs of CIP and LEV were determined.

Strain	MIC ($\mu\text{g/ml}$)		Ratio*		Ratio†	
	CIP	LEV	CIP	LEV	CIP	LEV
WT	0.015625	0.0625	1	1	N.D	N.D
285	2	2	128	32	N.D	N.D
287	4	4	256	64	N.D	N.D
285 $\Delta tolC$	0.125	0.0625	8	1	N.D	N.D
287 $\Delta tolC$	0.25	0.125	16	2	N.D	N.D
285 + 2319	0.125	0.25	8	4	1	4
287 + 2319	0.25	0.25	16	4	1	2

WT, *E. coli* AB1157

285 + 2319 and 287 + 2319, MIC values for *E. coli* 285 and 287 were determined in the presence of 25 μM MBX2319.

*, MIC ratio is equal to the $\text{MIC}_{\text{mutant or +2319}} / \text{MIC}_{\text{WT(AB1157)}}$.

†, MIC ratio is equal to the $\text{MIC}_{285 + 2319} / \text{MIC}_{285\Delta tolC}$ or $\text{MIC}_{287 + 2319} / \text{MIC}_{287\Delta tolC}$. N.D., not determined.

Table S2. *E. coli* strains 285 and 287 exhibit reduced susceptibility to multiple classes of antibacterial agents as compared to AB1157 (WT).

Drug	MIC ($\mu\text{g/ml}$)			Ratio (Mut/WT)	
	AB1157	285	287	285	287
Ciprofloxacin	0.016	1	2	64	128
Levofloxacin	0.063	2	4	32	64
Piperacillin	2	8	16	4	8
Amoxicillin	8	8	8	1	1
Cefotaxime	0.031	0.5	1	16	32
Tetracycline	1	4	8	4	8
Gentamicin	2	4	4	2	2
Chloramphenicol	4	16	32	4	8

Table S3. Nitrocefin hydrolysis in *E. coli* HN1159 (HN1167, $\Delta acrAB$) in the presence of polymyxin B nonapeptide (PMBN) and MBX2319. Unlike the cationic peptide PMBN, MBX2319 does not increase the rate of nitrocefin hydrolysis, indicating it does not perturb the outer membrane. The experiment was performed as described (3).

Compound	Conc.	nitrocefin hydrolysis rate, V_h (nmol/s/mg)		Percent Control
		Mean (N=3)	StDev	
none	0	0.0172	0.0000	100
PMBN	20 μ g/ml	0.0298	0.0018	174
MBX2319	0.2 μ M	0.0181	0.0008	106
MBX2319	2 μ M	0.0176	0.0005	102
MBX2319	*20 μ M	0.0168	0.0003	98

*compound was slightly above the solubility limit in assay buffer

Figure S1. *E. coli* 285 and 287 exhibit increased efflux activity as compared to AB1157 (WT) in the H33342 accumulation assay. **A)** *E. coli* 285. **B)** *E. coli* 287.

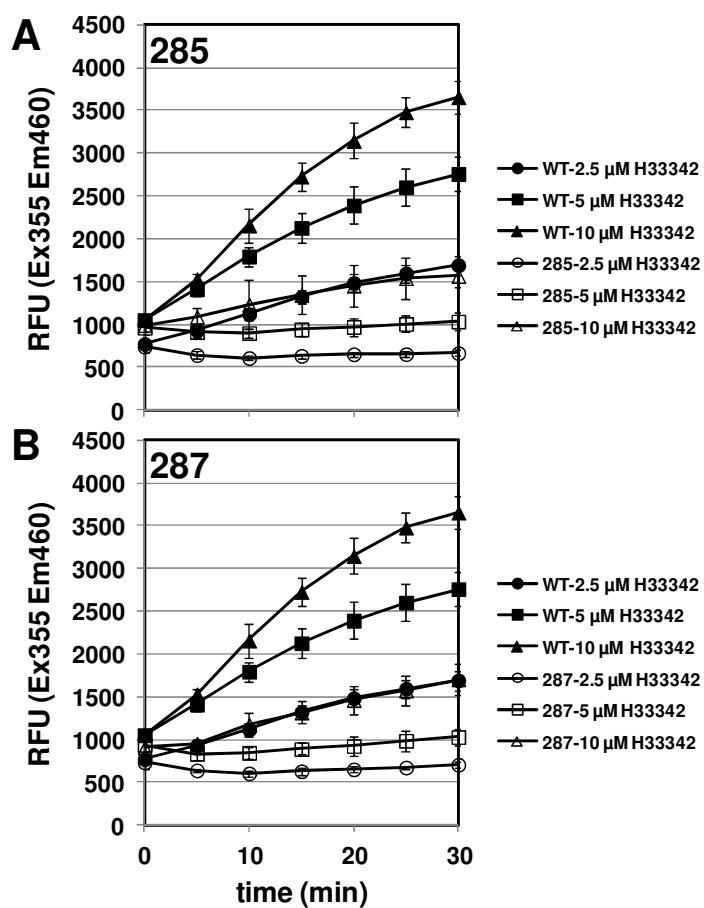


Figure S2. A comparison of the amino acid sequence of the Quinolone Resistance Determining Region (QRDR) of GyrA (amino acid residues 60-120) in *E. coli* AB1157 (WT), isogenic efflux over-expressing strains 285 and 287, and the reference strain MG1655.

```

                67                81 83  87                106
                x                x x   x                x
MG1655  60  NLAYKKSARVVGDVIGKYHPHGDSAVTDTIVRMAQPFFSLRYMLVDGQGNFGSIDGDSAAAM 120
AB1157  60  NKAYKKSARVVGDVIGKYHPHGDSAVYDTIVRMAQPFFSLRYMLVDGQGNFGSIDGDSAAAM 120
285     60  NKAYKKSARVVGDVIGKYHPHGDSAVYYTIVRMAQPFFSLRYMLVDGQGNFGSIDGDSAAAM 120
287     60  NKAYKKSARVVGDVIGKYHPHGDSAVYYTIVRMAQPFFSLRYMLVDGQGNFGSIDGDSAAAM 120

```

Summary of amino acid substitutions in the QRDR of GyrA of SOS-3 and isogenic ciprofloxacin-resistant mutants.

	Amino acid substitutions		
Strain	L55	T86	D87
MG1655	----	----	----
SOS-3 (WT)	L61K	T86Y	----
SOS-285	L61K	T86Y	D87Y
SOS-287	L61K	T86Y	D87Y

Table S4. *E.coli* strain panel used for cumulative MIC experiment.

Name	Description	Source (Reference)
AB1157	lab strain	(4)
ATCC 700336	UTI isolate	ATCC
ECOR-11	UTI isolate	ECOR Collection (5)
ECOR-14	UTI isolate	ECOR Collection (5)
ECOR-35	UTI isolate	ECOR Collection (5)
ECOR-38	UTI isolate	ECOR Collection (5)
ECOR-40	UTI isolate	ECOR Collection (5)
ECOR-48	UTI isolate	ECOR Collection (5)
ECOR-50	UTI isolate	ECOR Collection (5)
ECOR-55	UTI isolate	ECOR Collection (5)
ECOR-60	UTI isolate	ECOR Collection (5)
ECOR-62	UTI isolate	ECOR Collection (5)
ECOR-63	UTI isolate	ECOR Collection (5)
ECOR-64	UTI isolate	ECOR Collection (5)
ECOR-71	UTI isolate	ECOR Collection (5)
ECOR-72	UTI isolate	ECOR Collection (5)
PUTI 308	UTI isolate	BEI Resources*
MS110-3	colitis	BEI Resources*
ZK57	UTI isolate	(6)
O157:H7	stool VTEC	BEI Resources*
EH1533	stool VTEC	BEI Resources*
BAA-457	UTI isolate	ATCC
83972	asymptomatic bacteraemia	BEI Resources*
PUTI 026	UTI isolate	BEI Resources*
CFT073	UTI isolate	BEI Resources* (7)

Abbreviations: UTI, urinary tract infection; VTEC, verocytotoxin producing *E. coli*; ATCC, American Type Culture Collection, Manassas, VA.

*, Obtained through BEI Resources, NIAID, NIH.

Literature Cited

1. **Hunt JC, Briggs E, Clarke ED, Whittingham WG.** 2007. Synthesis and SAR studies of novel antifungal 1,2,3-triazines. *Bioorg Med Chem Lett* **17**:5222-5226.
2. **Paronikyan EG, Noravyan AS.** 1999. Synthesis of Fused Thiopyrans and Pyridines on the Base of Six-Membered Saturated Heterocycles. *Chem. Heterocycl. Comp* **35**:799-803.
3. **Nagano K, Nikaido H.** 2009. Kinetic behavior of the major multidrug efflux pump AcrB of *Escherichia coli*. *Proc Natl Acad Sci U S A* **106**:5854-5858.
4. **Dewitt SK, Adelberg EA.** 1962. The Occurrence of a Genetic Transposition in a Strain of *Escherichia Coli*. *Genetics* **47**:577-585.
5. **Ochman H, Selander RK.** 1984. Standard reference strains of *Escherichia coli* from natural populations. *J Bacteriol* **157**:690-693.
6. **Barondess JJ, Beckwith J.** 1995. bor gene of phage lambda, involved in serum resistance, encodes a widely conserved outer membrane lipoprotein. *J Bacteriol* **177**:1247-1253.
7. **Welch RA, Burland V, Plunkett G, 3rd, Redford P, Roesch P, Rasko D, Buckles EL, Liou SR, Boutin A, Hackett J, Stroud D, Mayhew GF, Rose DJ, Zhou S, Schwartz DC, Perna NT, Mobley HL, Sonnenberg MS, Blattner FR.** 2002. Extensive mosaic structure revealed by the complete genome sequence of uropathogenic *Escherichia coli*. *Proc Natl Acad Sci U S A* **99**:17020-17024.